pH and Driving Force Dependence of Intramolecular Oxyferryl Heme Reduction in Myoglobin

Craig W. Fenwick,[†] Ann M. English,*[,†] and James F. Wishart*[,‡]

Contribution from the Department of Chemistry and Biochemistry, Concordia University, 1455 de Maisonneuve Boulevard West, Montreal, Quebec H3G 1M8, Canada, and Department of Chemistry, Brookhaven National Laboratory, Upton, New York 11973-5000

Received September 4, 1996[⊗]

Abstract: The kinetics of oxyferryl (Fe^{IV}=O) heme reduction in horse heart myoglobin (Mb) by a_4LRu^{II} (a = NH_3; L = NH_3, pyridine, isonicotinamide) bound at the surface His48 were investigated with pulse radiolysis. The observed first-order rate constants (k_{obs1}) decreased with increasing pH and reduction potential for the a_4LRu centers ($E°/Ru^{III/II}$ = 77, 330, and 400 mV for L = NH_3, Pyr, and Isn). Rate−pD data obtained in D_2O for the a_5Ru derivative revealed the presence of an equilibrium isotope effect, and a pK_a of 5.7 (6.2 in D_2O) was obtained for the acid−base group, which is assigned to the distal His64. A mechanism where protonation *precedes* ET provides a good fit of the kinetic data for the three a_4LRu derivatives. Marcus theory analysis of the k_{ET} (0.74, 1.8, and 3.6 s^{-1} for L = Isn, Pyr, and NH_3) extracted from the k_{obs1} values yielded a reorganization energy (λ) of 1.8 for $Ru^{II} \rightarrow Fe^{IV}$=O ET in the a_4LRu derivatives but a λ of 2.1 eV for the a_5Ru derivative. From the latter, it is concluded that ET is strongly gated in the a_5Ru derivative, and this is assumed to be the major reason for the low reactivity of Fe^{IV}=O in Mb at high $-\Delta G°$.

Introduction

In recent years it has been found or hypothesized that all heme enzymes involved in redox catalysis use an oxyferryl (Fe^{IV}=O) heme in their catalytic cycles.[1,2] Fe^{IV}=O centers have oxidizing potentials close to 1 V and their reduction *in vivo* is coupled to a multitude of reactions.[2] These include those reactions carried out by cytochromes P_{450} in drug metabolism and detoxification in the liver, in the breakdown of lignin by lignin peroxidase, and in the reduction of O_2 to H_2O by cytochrome *c* oxidase. Despite the importance and scope of these heme enzymes, relatively little is known about what factors control the reactivity of Fe^{IV}=O centers in proteins. These centers are best characterized in heme peroxidases[2] where they are generated on the rapid reaction ($\geq 10^7$ M^{-1} s^{-1}) of the ferric enzymes (Fe^{III},P) with H_2O_2:

$$Fe^{III},P + H_2O_2 \rightarrow Fe^{IV}{=}O,P^{\bullet+} + H_2O \qquad (1a)$$

$$Fe^{IV}{=}O,P^{\bullet+} + 1e^- \rightarrow Fe^{IV}{=}O,P \qquad (1b)$$

$$Fe^{IV}{=}O,P + 1e^- + 2H^+ \rightarrow Fe^{III},P + H_2O \qquad (1c)$$

The two-electron oxidized intermediate generated in (1a) is termed compound **I**, where $P^{\bullet+}$ is a cation radical located either on the porphyrin or protein.[2] Compound **I** is generally reduced back to the resting form in one-electron steps via compound **II**.[2]

Myoglobin (Mb) is a small (MW ∼17 kDa), stable heme protein designed to reversibly bind dioxygen.[3] When exposed to H_2O_2, it reacts slowly ($\sim 10^2$ M^{-1} s^{-1})[4] to form a stable Fe^{IV}=O heme and a protein radical that decays quickly[4,5] without causing detectable modification to the polypeptide.[6] Oxyferryl Mb ($MbFe^{IV}$=O) has been extensively characterized;[4,5,7] hence, the study of $MbFe^{IV}$=O reactivity is informative since there are obvious structural differences between Mb and heme peroxidases. In particular, the solvent-isolated, hydrophobic heme pocket of Mb[8a] contrasts sharply with the peroxidase active site, which contains a number of H_2O molecules and is linked by a hydrated channel to the solvent.[8b] This water bridge can provide a source of protons to facilitate the rapid reduction of the oxene ligand (eq 1c), which appears to be the rate-limiting step in peroxidase turnover.[9] The goal of this work is to probe the electron-transfer (ET) reactivity of the Fe^{IV}=O heme center in horse heart Mb (HHMb). The reaction of interest is the following:

* Authors to whom correspondence should be addressed
† Concordia University.
‡ Brookhaven National Laboratory.
⊗ Abstract published in *Advance ACS Abstracts,* May 1, 1997.

(1) (a) Mueller, E. J.; Loida, P. J.; Sligar, S. G. In *Cytochrome P450 Structure, Mechanism and Biochemistry*, 2nd ed.; Ortiz de Montellano, P. R., Ed.; Plenum Press: New York, 1995; pp 83−124. (b) Poulos, T. L.; Cupp-Vickery, J.; Li, H. In *Cytochrome P450 Structure, Mechanism and Biochemistry*, 2nd ed.; Ortiz de Montellano, P. R., Ed.; Plenum Press: New York, 1995; pp 125−150. (c) Babcock, G. T.; Wilkström, M. *Nature* **1992**, *356*, 301. (d) Malmström, B. G. *Acc. Chem. Res.* **1993**, *26*, 332.

(2) (a) English, A. M.; Tsaprailis, G. *Adv. Inorg. Chem.* **1995**, *43*, 79. (b) Poulos, T. L. *Adv. Inorg. Biochem.* **1987**, *7*, 1. (c) Poulos, T. L.; Fenna, R. E. In *Metal Ions in Biological Systems: Metalloenzymes Involving Amino Acid-Residue and Related Radicals*; Sigel, H., Sigel, A., Eds.; Marcel Dekker: New York, 1994; Vol. 30, pp 25−75.

(3) Springer, B. A.; Sligar, S. G.; Olson, J. S.; Phillips G. N., Jr. *Chem. Rev.* **1994**, *94*, 699.

(4) Yonetani, T.; Schleyer, H. *J. Biol. Chem.* **1967**, *242*, 1974.

(5) (a) King, N. K.; Winfield, M. E. *J. Biol. Chem.* **1963**, *238*, 1520. (b) Davies, M. J. *Biochim. Biophys. Acta.* **1991**, *1077*, 86.

(6) Peptide mass mapping by LC-MS of horse heart Mb after exposure to 10 molar equiv of H_2O_2 revealed no mass-modified peptides compared to untreated Mb (C. W. Fenwick, to be submitted for publication).

(7) (a) George, P.; Irvine, D. H. *Biochem. J.* **1952**, *52*, 511. (b) King, N. K.; Winfield, M. E. *Aust. J. Biol. Sci.* **1966**, *19*, 211. (c) Fox, J. B.; Nicholas, R. A.; Ackerman. S. A.; Swift, C. E. *Biochemistry* **1974**, *13*, 5178. (d) Wittenberg, J. B. *J. Biol. Chem.* **1978**, *253*, 5694; (e) Peisach, J.; Uyeda, M. *Biochemistry* **1981**, *20*, 2028. (f) Foote, N.; Gadsby, P. M. A.; Greenwood, C.; Thomson, A. J. *Biochem. J.* **1989**, *261*, 515.

(8) (a) Quillin, M. L.; Arduini, R. M.; Olson, J. S.; Phillips, G. N., Jr. *J. Mol. Biol.* **1993**, *234*, 140. (b) Finzel, B. C.; Poulos, T. L.; Kraut, J. *J. Biol. Chem.* **1984**, *259*, 13027.

(9) (a) Miller, M. A.; Vitello, L.; Erman, J. E. *Biochemistry* **1995**, *34*, 12048. (b) Farhangrazi, Z. S.; Fossett, M. E.; Powers, L. S.; Ellis, W. R., Jr. *Biochemistry* **1995**, *34*, 2866. (c) Hahm, S.; Miller, M. A.; Geren, L.; Kraut, J.; Durham, B.; Millett, F. *Biochemistry* **1994**, *33*, 1473. (d) Hasinoff, B. B.; Dunford, H. B *Biochemistry* **1970**, *9*, 4930.

S0002-7863(96)03108-3 CCC: $14.00

$$MbFe^{IV}{=}O + 1e^- + 2H^+ \rightarrow MbFe^{III}{-}OH_2 \qquad (2)$$

Reaction 2 differs from that in (1c) in that the H_2O generated on reductive protonation of the oxene ligand remains bound to the Fe^{III} center in Mb. To eliminate the uncertainties associated with bimolecular ET reactions, intramolecular reduction was performed by modifying the surface His48 of HHMb with redox-active Ru complexes following well-established protocols.[10−13] ET rates have been extensively studied in Fe^{II}, Fe^{III}, and metalloderivatives of sperm whale Mb (SWMb) with this methodology.[10,11] We have reported previously that the reaction $a_5Ru^{II} \rightarrow Fe^{IV}{=}O$ ET in HHMb is surprisingly slow.[14] To gain further insight into the mechanism of this latter reaction, the ligands of the bound Ru complex were changed to determine the effects of varying the driving force for ET on the observed rates. The reactions were also carried out in H_2O and D_2O as a function of pH/pD to investigate the mechanism of proton involvement in the reductive protonation of $Fe^{IV}{=}O$ to $Fe^{III}{-}OH_2$ (eq 2).

Experimental Section

Materials. Horse heart myoglobin (HHMb) and bovine liver catalase were purchased from Sigma, and modified sequencing-grade trypsin was purchased from Boehringer Mannhein. Chemicals were obtained from the following suppliers: chloro(pentaammine)ruthenium(III) chloride ($a_5Ru^{III}Cl)Cl_2$ (Johnson Matthey); $CoCl_2{\bullet}6H_2O$, pyridine, isonicotinamide, 4,4′-bipyridine, and 1,10-phenanthroline monohydrate (Aldrich); KCN (BDH Chemicals); buffer salts, HCOONa, 30% H_2O_2 (Fisher); 99.8% D_2O (Brookhaven). Chloro(tetraammine)(pyridine)ruthenium(III) chloride ($a_4Ru^{III}PyrCl)Cl_2$, chloro(tetraammine)(isonicotinamide)ruthenium(III) chloride ($a_4Ru^{III}IsnCl)Cl_2$,[15a−c] and tris(1,10-phenanthroline)cobalt(III) chloride $[Co(phen)_3^{3+}]$[15d] were synthesized by the literature procedures, as were the a_4LRuHis model complexes.[16] Zinc amalgam was prepared by adding acid (1 mM HCl) washed Zn granules (Fisher) to a saturated solution of mercuric chloride (Mallinckrodt), stirring over low heat for 10 min, washing with distilled water, and air drying. Sephadex G-25 gel-filtration resin was purchased from Pharmacia, and a stirred ultrafiltration cell and YM 5 membranes (5000 MW cutoff) were purchased from Amicon.

Methods. Derivatization of the surface histidines of HHMb with the Ru complexes was performed by following the published procedures[10] with slight modifications. Solutions containing 1 mM HHMb and 30 mM $a_4LRu^{III}Cl$ (L = NH_3, pyridine, or isonicotinamide) in 50 mM Tris buffer (pH 7.0) were separately degassed under a constant flow of argon for 1 h. Freshly prepared Zn amalgam was added to the $a_4LRu^{III}Cl$ solution and the $a_4LRu^{II}H_2O$, which formed under argon in ∼1.5 h, was transferred by gas-tight syringe to the Mb sample. The resulting solution, which contained 11 mM Ru^{II} complex and 0.6 mM Mb, was left standing for 1 h at room temperature, and excess Ru complex was removed by gel filtration on a G-25 column (2.5 × 40 cm) under anaerobic conditions. The protein was eluted first as a dark red band, the Fe^{II} and Ru^{II} centers were immediately oxidized with $Co(phen)_3^{3+}$, and the oxidant was removed by ultrafiltration with 50 mM NaPi buffer (pH 6.0). The Mb derivatives were separated on a cation-exchange column (Mono S HR 10/10, Pharmacia) fitted to a Pharmacia FPLC system. The FPLC-separated Mb derivatives were characterized by UV/vis spectroscopy and electrospray mass spectrometry (ES-MS). For UV/vis analysis, a 5 μM $a_4LRu^{III}MbFe^{III}$ solution was reacted with excess KCN to form the $Fe^{III}{-}CN$ complex, and sufficient sodium ascorbate was added to reduce the Ru^{III} but not the $Fe^{III}{-}CN$ center. The a_4LRu^{III} minus a_4LRu^{II} difference spectra were recorded on a Beckman DU 650 spectrophotometer and compared to those of the free a_4LRuHis complexes to identify the FPLC bands containing native and singly- and multiply-modified Mb.

Prior to ES-MS, 2 μg of FPLC-purified Mb derivative was desalted on a Vydac C18 HPLC column (4.6 × 250 mm) with use of a linear (10−60%) CH_3CN gradient in 0.1% TFA over 15 min at a flow rate of 1 mL/min. ApoMb was eluted at ∼50% CH_3CN, lyophilized, resuspended in 1:1 methanol−water with 0.5% acetic acid, and infused at 2 μL/min into the ES source of a Finnigan SSQ 7000 mass spectrometer.

The site of Ru attachment in the singly-modified Mb derivatives was identified by tryptic digestion followed by on-line LC-MS. ApoMb (10 μM) was digested with 1:50 (w/w) trypsin in 0.1 M $NaHCO_3$ at 37 °C for 4 h, and digestion was stopped by lowering the pH to 2 with acetic acid. A 5-μL aliquot was loaded on a Vydac C18 microbore column (1 × 250 mm) fitted to a HP 1090 HPLC system, and the tryptic peptides were separated with use of a linear (0 −60%) CH_3CN gradient in 0.05% TFA over 60 min at a flow rate of 40 μL/min. The effluent was fed directly into the mass spectrometer to identify the peptides with a bound a_4LRu group.

Reduction potentials ($E°'$) of the Mb-bound Ru^{III} complexes were determined by differential pulse voltammetry (DPV) with use of a BAS 100A potentiostat. A 1-mL solution containing 50 μM $a_4LRu^{III}Mb$ and 10 mM 4,4′-bipyridine in 50 mM NaPi (pH 7.0) was degassed under N_2 for 15 min in a sealed electrochemical cell with a gold working electrode, Ag/AgCl reference electrode (BAS), and Pt wire (Fisher) auxiliary electrode before measurements were taken. Addition of 4,4′-bipyridine promoted heterogenous ET between the gold electrode and Mb and minimized irreversible protein adsorption on the electrode.[17]

ET was initiated by electron pulse radiolysis with a 2-MeV Van de Graaff accelerator at Brookhaven as previously described.[14,18] Derivatized Mb samples (0.5−2 μM) were prepared in 40 mM NaPi buffer containing 12 mM HCOONa and saturated with N_2O gas. The formate ion reacts with radiolytically-generated $OH^•$ to give $CO_2^{•-}$:

$$H_2O \rightsquigarrow e^-_{aq} + OH^• + H^+ \qquad (3a)$$

$$e^-_{aq} + N_2O + H_2O \rightarrow N_2 + OH^• + OH^- \qquad (3b)$$

$$OH^• + HCO_2^- \rightarrow CO_2^{•-} + H_2O \qquad (3c)$$

$CO_2^{•-}$ is a strong reductant ($E° = -1.90$ V vs NHE)[19] that reduces the metal centers without damaging the protein. The electron dose in each pulse was chosen to generate sufficient $CO_2^{•-}$ to reduce ≤10% of the protein[14] in 2.0 or 6.1 cm path length cells at 25 °C. $Ru^{II} \rightarrow$ heme ET was followed by monitoring changes in the Soret band of Mb ($Fe^{IV}{=}O$, $\epsilon_{421} = 111$ mM^{-1} cm^{-1}; $Fe^{III}{-}H_2O$, $\epsilon_{409} = 188$ mM^{-1} cm^{-1}; Fe^{II}, $\epsilon_{434} = 135$ mM^{-1} cm^{-1}).[14]

$Fe^{IV}{=}O$ samples were prepared by reacting 200−400 μM $MbFe^{III}{-}H_2O$ with 5-fold excess H_2O_2 in argon degassed reaction buffer at pH 7.0. When $MbFe^{IV}{=}O$ was fully formed (as determined spectrophotometrically), a catalytic amount of catalase was added to remove excess H_2O_2, and an aliquot transferred by gas-tight syringe to the pulse radiolysis cell containing N_2O-saturated reaction buffer. The pH was adjusted by adding stock $MbFe^{IV}{=}O$ at pH 7.0 to a buffer of lower or higher pH in the cell, and the pH of pulsed and unpulsed samples was monitored to assure sufficient buffering during the kinetic measure-

(10) (a) Crutchley, R. J.; Ellis, W. R., Jr.; Gray, H. B. *J. Am. Chem. Soc*. **1985**, *107*, 5002. (b) Lieber, C. M.; Karas, J. L.; Gray, H. B. *J. Am. Chem. Soc*. **1987**, *109*, 3778. (c) Axup, A. W.; Albin, M.; Mayo, S. L.; Crutchley, R. J.; Gray, H. B. *J. Am. Chem. Soc.* **1988**, *110*, 435. (d) Karas, J. L.; Lieber, C. M.; Gray, H. B. *J. Am. Chem. Soc*. **1988**, *110*, 599. (e) Karas, J. L. Ph.D. Thesis, California Institute of Technology, 1989.

(11) Winkler, J. R.; Gray, H. B. *Chem. Rev.* **1992**, *92*, 369.

(12) Isied, S. S. In *Electron Transfer in Inorganic, Organic and Biological Systems*; Bolton, J. R., Mataga, N., McLendon, G., Eds.; Advances in Chemistry Series No. 228; American Chemical Society: Washington, DC, 1991; pp 229−245.

(13) Sykes, A. G. *Chem. Br.* **1988**, *June*, 551.

(14) Fenwick, C.; Marmor, S.; Govindaraju, K.; English, A. M; Wishart, J. F.; Sun, J. *J. Am. Chem. Soc.* **1994**, *116*, 3169.

(15) (a) Vogt, L. H., Jr.; Katz, J. L.; Wiberley, S. E. *Inorg. Chem.* **1965**, *4*, 1157. (b) Curtis, J. C.; Sullivan, B. P.; Meyer, T. J. *Inorg. Chem.* **1983**, *22*, 224. (c) Marchant, J. A.; Matsubara, T.; Ford, P. C. *Inorg. Chem.* **1977**, *16*, 2160. (d) Schlit, A. A.; Taylor, R. C. *Russ. J. Inorg. Chem. (Engl. Transl.)* **1959**, *9*, 211.

(16) Sundberg, R. J.; Gupta, G. *Bioinorg. Chem.* **1973**, *3*, 39.

(17) (a) Eddowes, M. J.; Hill, H. A. O. *J. Chem. Soc., Chem. Commun.* **1977**, 771. (b) Eddowes, M. J.; Hill, H. A. O.; Uosaki, K. *Bioelectrochem. Bioenerg.* **1980**, *7*, 527.

(18) Sun, J.; Su, C.; Wishart, J. F. *Inorg. Chem.* **1996**, *35*, 5893.

(19) Schwartz, H. A.; Dodson, R. W. *J. Phys. Chem.* **1989**, *93*, 409.

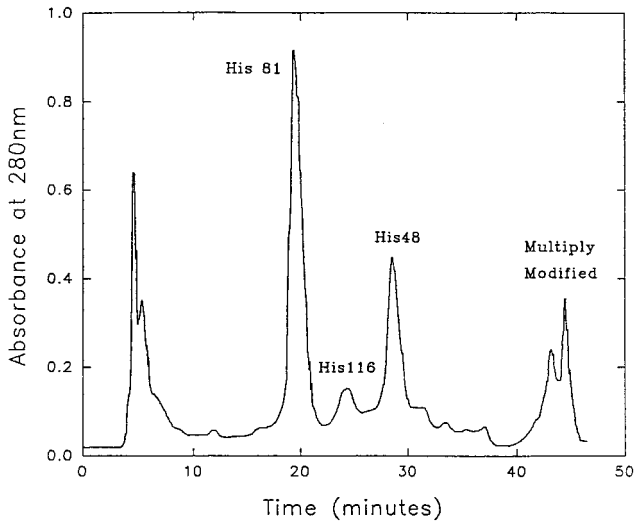

Figure 1. Separation of a_4IsnRuMb derivatives by cation-exchange FPLC. The Mono S HR 10/10 column was equilibrated with 50 mM NaPi, pH 7.0, and ~500 μL of 1 mM (17 mg/ml) Mb was loaded on the column and the components separated with use of a linear gradient NaCl (0 to 200 mM) in 50 mM NaPi, pH 7.0, with a flow rate of 0.6 mL/min, fraction size 0.5 mL. The elution was monitored at 280 nm, and each peak was collected and saved for analysis. The peaks containing Mb singly derivatized at the three surface histidines are labeled.

ments. Samples in D_2O were equilibrated overnight before use to allow complete H/D exchange at room temperature. The pD (= pH + 0.4)[20] was controlled in the same way as the pH, and extreme care was taken to minimize introduction of H^+. Kinetic measurements were performed immediately after $MbFe^{IV}$=O formation since this species spontaneously decays back to $MbFe^{III}-OH_2$ ($t_{1/2}$ ~66 min at pH 6.5 and <16 min at pH 5.6).

Results

Purification of the ruthenation reaction mixtures by cation-exchange FPLC (Figure 1) allowed isolation and separation of the singly-modified HHMb derivatives as previously reported for SWMb.[10] Native HHMb was eluted first from the Mono S column, followed by singly- and multiply modified samples. Derivatives singly-modified at the surface histidines (48, 81, and 116) were obtained in 8−15% yield. His48-modified HHMb was the last of the singly-modified derivatives to be eluted from the FPLC column for each Ru complex.

ES-MS confirmed the UV/vis results that singly-modified derivatives with covalently-bound a_4LRu had been prepared. The deconvoluted mass spectrum of a_4IsnRuHis48Mb is shown in Figure 2, with the major peak at 17 237 corresponding to that of the apo form, since the heme dissociates from the globin under the acidic ES-MS conditions.[21] A phosphate adduct of a_4IsnRuHis48Mb is observed at 17 335, and adduct dissociation occurs at higher voltages. The spray voltage in the ES source was maintained at <3.7 kV, otherwise fragmentation of the bound Ru complex occurred during ionization. Even under the soft ionization conditions used, peaks corresponding to apoMb and apoMb + Ru are evident in Figure 2.

Reduction potentials for the HHMb-bound a_4LRu^{III}His groups were determined since the protein environment is known to shift the $E^{o\prime}$ values of the Ru complexes from those measured for the corresponding free complexes.[22] Peak potentials (E_p) were measured at several different pulse amplitudes (ΔE) for each

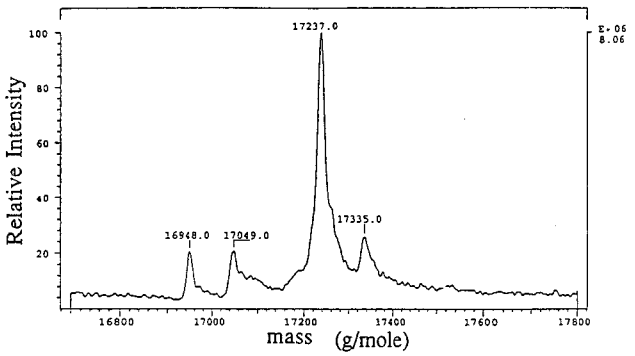

Figure 2. Deconvoluted ES mass spectrum of a_4IsnRuHis48Mb. The lyophilized sample (<1 μg) dissolved in 50 μL of methanol−H_2O with 0.5% acetic acid was infused into the ES source at a flow rate of 2 μL/min. The spray voltage was maintained at 3.7 kV to avoid dissociation of the Ru complex (see text). The peaks at mass 17 237 and 17 335 correspond to the heme-free form of a_4IsnRuHis48Mb and a phosphate adduct, and those at 16 948.0 and 17 049.0 correspond to apoMb and apoMb plus Ru.

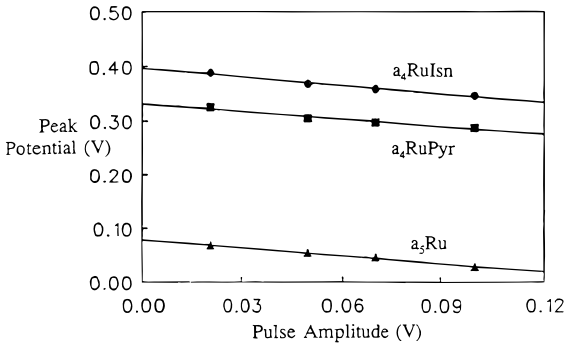

Figure 3. Differential pulse voltammetry of the Ru^{III} center of a_4-LRuHis48Mb (40−100 μM) in N_2-saturated 50 mM NaPi (pH 7.0) containing 10 mM 4,4′-bipyridine. The potential of the gold working electrode (vs Ag/AgCl) was scanned at 5 mV/s, and the data points represent peak potentials of $Ru^{III/II}$ (vs NHE) at different pulse amplitudes. The $E^{o\prime}$ values were calculated from eq 4 in the text.

Table 1. Reduction Potentials (mV vs NHE) for $Ru^{III/II}$ in Free and Protein-Bound a_4LRuHis Complexes[a]

a_4LRu group	model complex[b]	HHMb[b] His48	SWMb[c] His48	Ck Cyt *c*[d] His39	HH Cyt *c*[d] His33
a_5Ru	71 ± 2	77 ± 1	85	95	128
a_4PyrRu	309 ± 3	330 ± 3	340	−	370
a_4IsnRu	388 ± 3	400 ± 2	420	400	434

[a] Phosphate buffer (pH 7.0) with 10 mM 4,4′-bipyridine. [b] This work (see Figure 3). [c] Sperm whale Mb data from refs 10a and 10e. [d] *Candida krusei* and horse heart cyts *c* data from ref 49.

Mb derivative, and $E^{o\prime}$ values were determined from:[23]

$$E_p = E^{\circ\prime} - \frac{\Delta E}{2} \qquad (4)$$

Slopes of E_p vs ΔE plots (Figure 3) were close to the predicted value of −0.5, and the *y* intercepts yielded $E^{o\prime}$ values of 77, 330, and 400 mV for a_5RuHis48Mb, a_4PyrRuHis48Mb, and a_4-IsnRuHis48Mb, respectively. These values are compared in Table 1 to those found for the free model complexes and to literature values for other heme proteins. Interestingly, the $E^{\circ\prime}$ values for the Ru^{III} centers bound to His48 of HHMb are 8−20 mV lower than those bound to His48 of SWMb.

(20) Schowen, K. B. J. In *Transition States of Biochemical Processes*; Gandour, R. D., Schowen, R. L., Eds.; Plenum Press: New York, 1978; pp 225−283.
(21) Feng, R.; Konishi, Y. *J. Am. Soc. Mass. Spectrom.* **1993**, *4*, 638.
(22) Bowler, B. E.; Raphael, A. L.; Gray, H. B. *Prog. Inorg. Chem.* **1990**, *38*, 259.
(23) Bard, A. J.; Faulkner, L. R. In *Electrochemical Methods*; John Wiley & Sons: New York, 1980; p 194.

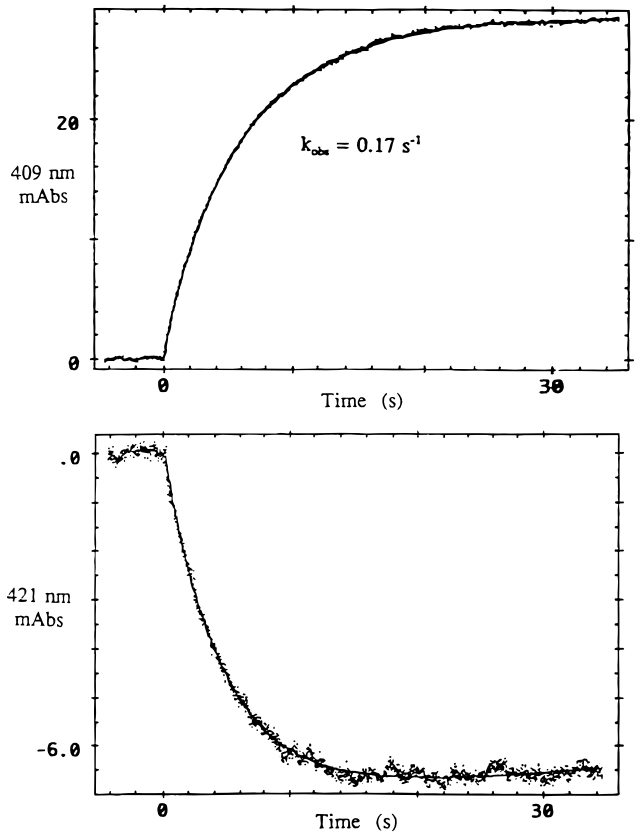

Figure 4. Observed absorbance change at 409 nm ($Fe^{III}-OH_2$ formation) and 421 nm ($Fe^{IV}=O$ decay) vs time following pulse radiolysis of 1 μM $a_5Ru^{III}His48MbFe^{IV}=O$ in N_2O-saturated 40 mM NaPi, 12 mM HCOONa (pH 7.0) at room temperature, path length 2 cm. A 60-ns electron pulse was applied at $t = 0$ and the dose used was sufficient to reduce <10% of the Ru^{III} centers. The solid lines show the fit of the experimental points to first-order kinetics.

Following the electron pulse, the $CO_2^{\bullet-}$ radical rapidly ($k > 10^9$ M^{-1} s^{-1}) and preferentially (>95%) reduced the Ru centers of $a_4LRu^{III}MbFe^{IV}=O$.[24] $Ru^{II} \rightarrow Fe^{IV}=O$ ET was readily followed on the second time scale by monitoring the absorbance increase at 409 nm on $MbFe^{III}-OH_2$ formation, or the decrease at 421 nm on $MbFe^{IV}=O$ decay. The rate data were analyzed by fitting the absorbance changes by competing first- and second-order processes. At pH $\leq$7, the amplitude of the second-order process was negligible at the low concentration of protein used, and the data are well fit by the first-order process alone (Figure 4), which is attributed to:

$$a_4LRu^{II}His48-Fe^{IV}=O + 2H^+ \xrightarrow{k_{obs1}} a_4LRu^{III}His48-Fe^{III}-OH_2 \quad (5)$$

The k_{obs1} values were independent of the initial a_4LRu^{II}-$His48MbFe^{IV}=O$ concentration (0.5−2.0 μM), indicating that $Fe^{IV}=O$ reduction occurs via intramolecular ET as indicated in eq 5, and as previously reported for $a_5Ru^{II}His48MbFe^{IV}=O$.[14] Above pH 7.5 the second-order process has significant amplitude, and dominates at pH 8 where the k_{obs1} values are $\leq$0.01 s^{-1}.

Figure 5 shows the k_{obs1}−pH and k_{obs1}−pD plots for a_5Ru^{II}-$His48MbFe^{IV}=O$, and the k_{obs1}−pH plots for the a_4LRu derivatives. The kinetics of $a_5Ru^{II}His48-Fe^{III}-OH_2 \rightleftharpoons a_5R^{III}$-

(24) The ratio of the rates for $CO_2^{\bullet-}$ radical reacting with the Ru^{III} and $Fe^{IV}=O$ centers was estimated from the absorbance growth at 409 nm due to $Fe^{III}-OH_2$ formation on millisecond (direct reduction by $CO_2^{\bullet-}$) and second (intramolecular ET from Ru^{II}) time scales.

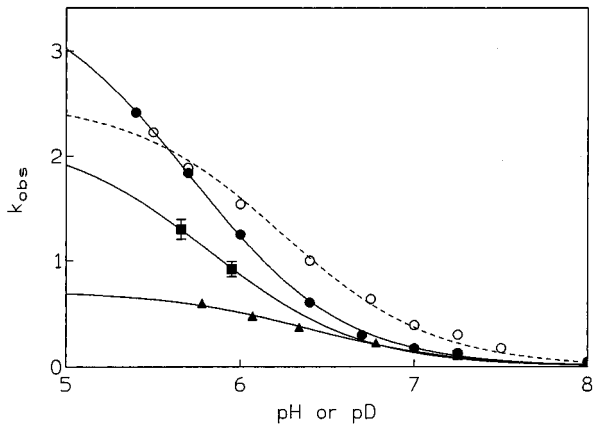

Figure 5. Variation of k_{obs1} with pH (pD) for the first-order reduction of $Fe^{IV}=O$ by surface-bound Ru^{II} in $a_4LRu^{II}His48MbFe^{IV}=O$. Experimental conditions are given in Figure 4. Fit of the experimental data by eq 6b in the text is given by the solid lines for the pH data and the dashed line for the pD data. The nonlinear least-squares analyses were carried out by using MINSQ Software (MicroMath). Closed circles, $a_5RuHis48Mb$ in H_2O; open circles, $a_5RuHis48Mb$ in D_2O; squares, $a_4PyrRuHis48Mb$ in H_2O; triangles, $a_4IsnRuHis48Mb$ in H_2O. Data points are the average of 4−8 kinetic runs.

Table 2. Analysis Using Eq 6b of k_{obs1} (s^{-1}) vs pH for $Fe^{IV}=O$ Reduction by Surface-Bound Ru^{II} in $a_4LRu^{II}His48MbFe^{IV}=O$[a]

a_4LRu group	pK_a	k_2 (s^{-1})	$-\Delta G°$ (eV)[b]
a_5Ru (in H_2O)	5.7	3.6	0.752
a_5Ru (in D_2O)	6.2	2.5	0.752
a_4PyrRu (in H_2O)	6.0	1.9	0.499
a_4IsnRu (in H_2O)	6.4	0.74	0.429

[a] Experimental details are given in Figure 3. [b] Kinetic driving force estimated for $Ru^{II} \rightarrow Fe^{IV}=O$ ET; see text.

His48−Fe^{II} + H_2O in HHMb were also examined at pH 7.0 and 5.4, and k_{obs1} values of 0.059 ± 0.003 and 0.063 ± 0.005 s^{-1}, respectively, were obtained. Since ET to the Fe^{III} heme is not a proton-coupled process, the pH independence of k_{obs1} suggests that the electronic coupling between the Ru^{II} and heme centers is also pH independent over the same range.

Discussion

Mechanism of $Fe^{IV}=O$ Reduction in a_4LRuMb. As Figure 5 reveals, the k_{obs1} values for intramolecular $Fe^{IV}=O$ reduction by Ru^{II} are greater in D_2O than H_2O for $a_5RuHis48Mb$ between pH ca. 5.8 and 7.5. This is indicative of an isotope effect arising from an acid−base equilibrium of a group on the protein, the pK_a of which will be elevated in D_2O.[20] The presence of an equilibrium isotope effect reveals that a protonated form of Mb is reactive in ET, suggesting the following mechanism:

$$a_4LRu^{II}-MbFe^{IV}=O + H^+ \underset{K_a}{\rightleftharpoons} a_4LRu^{II}-H^+MbFe^{IV}=O \xrightarrow{k_2} a_4LRu^{III}-MbFe^{III}-OH_2 \quad (6a)$$

$$k_{obs1} = \frac{k_2[H^+]}{K_a + [H^+]} \quad (6b)$$

Fitting the k_{obs1} values in Figure 5 by eq 6b yielded pK_a and k_2 values of 5.71 and 3.60 s^{-1} in H_2O, and 6.23 and 2.53 s^{-1} in D_2O for the a_5Ru derivative (Table 2). A ΔpK_a of 0.52 is within the range of equilibrium isotope effects predicted for acids of pK_a 3 −10,[20] and is assigned to the distal His64 of Mb since the imidazole side chain of this group interacts with heme ligands as discussed below.

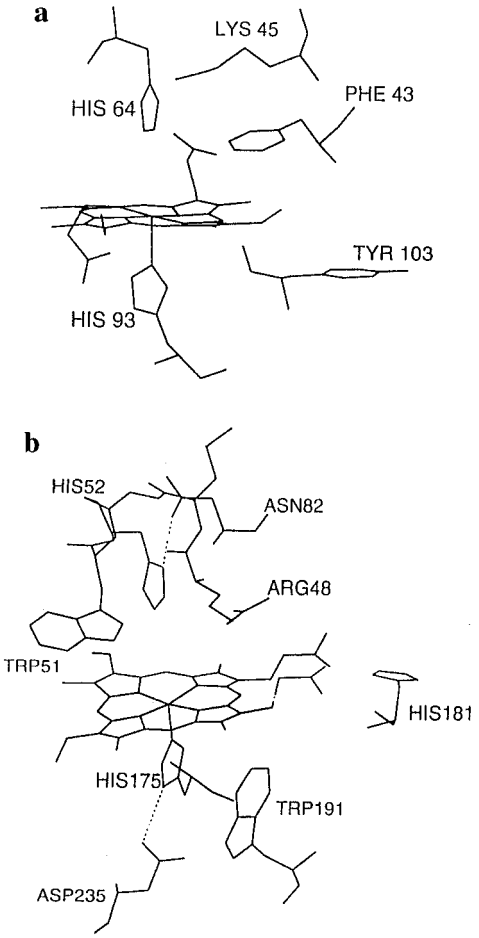

Figure 6. (a) Diagram of the heme pocket of Mb generated with use of the X-ray coordinates from the 1.9-Å structure of horse heart metMb.[26] (b) Heme pocket of cytochrome *c* peroxidase (CCP) showing the key catalytic residues. The dashed lines represent H-bonds. The diagram was generated with use of the X-ray coordinates from the 1.7-Å structure of CCP.[8b]

The fit by eq 6b of the k_{obs1} vs [H^+] data for the intramolecular reduction of Fe^{IV}═O in a_4PyrRuMb and a_4IsnRuMb was also carried out (Figure 5). The resultant k_2 values (Table 2) decreased as $E°/Ru^{III/II}$ increased (Table 1), indicating that ET is involved in the rate-limiting step following the preequilibrium in eq 6a. However, K_a was also found to be sensitive to ligand substitution in a_4LRu with pK_a = 5.7, 6.0, and 6.4 for L = NH_3, Pyr, and Isn, respectively. This variation in pK_a assigned to the *distal* His64 with a redox group bound at the *surface* His48 was unexpected, and the reasons for it are not obvious at the present time. Addition of an extra term in eq 6b corresponding to the rate constant for ET in the unprotonated form of Mb essentially has no effect on either the pK_a or k_2 values listed in Table 2.

In Mb the heme sits in the hydrophobic pocket shown in Figure 6a. Ligand access to the pocket requires fluctuations in the polypeptide structure,[25−27] which protects the O_2 ligand from protonation[3,28] and promotes reversible O_2 binding since the distal His64 at 4.3 Å from the iron[26] forms a stabilizing H-bond with the O_2 ligand.[3] Protonation of His64 increases accessibility to the heme[29,30] because the protonated form swings out toward the solvent, leaving the heme pocket in the open conformation observed by X-ray crystallography of Mb with bulky heme ligands.[31] CO on- and off-rates to the Fe^{II} heme are ∼10 times higher in the open-pocket compared to the closed-pocket conformations,[30] which interconvert on protonation of His64 with a pK_a of ∼6.[29] From the different Fe−C and CO stretching vibrations in the open and closed conformations,[29,30] $MbFe^{II}$−CO appears to be mainly in the closed-pocket conformation at neutral pH, but interconversion between the closed and open forms is reported to be fast (1−10 μs).[30]

A similar equilibrium may be important for Mb's physiological function since O_2 dissociation rates drastically increase ($10^{3\pm2}$ vs 13 s^{-1}) in the open-pocket vs closed-pocket forms of $MbFe^{II}$−O_2, facilitating O_2 delivery to muscle tissue at lower pH values.[30] $MbFe^{II}$−O_2 is also more susceptible to autoxidation at low pH.[28,32] The proposed mechanism for acid-catalyzed autoxidation involves proton transfer (PT) from the *protonated* distal His64 to the O_2 ligand, followed by displacement of $HO_2^•$ by an entering H_2O molecule to form $MbFe^{III}$−OH_2.[28,32] The H-bond provided by the NE2 atom of the *neutral* His64 stabilizes the O_2 ligand, preventing both its dissociation and protonation so that PT to the O_2 ligand is efficient only in the *acid* form of $MbFe^{II}$−O_2.[28,32]

Fe^{IV}═O reduction by mechanism 6a can be interpreted in terms of the pH-dependent processes involving the heme pocket of Mb. Species a_4LRu^{II}−H^+MbFe^{IV}═O is assumed to be an open-pocket conformation of Mb with the distal His64 protonated. The pK_a of this residue is ∼6 in the open-pocket form of $MbFe^{II}$−CO,[29] which agrees with the pK_a values predicted by mechanism 6a (Table 2).

Kinetic vs Thermodynamic Driving Force for ET. The thermodynamic potential for $MbFe^{IV}$═O reduction to $MbFe^{III}$−OH_2 is 0.896 eV (vs NHE) at pH 7.[33a] Equilibrium measurements of $E°'$ vs pH reveal the uptake of two protons[33b] below the pK_a of $HHMbFe^{III}$−OH_2 (8.93).[34] Since the ET reactions were carried out at pH values below the pK_a, the observed product possessed H_2O as a ligand rather than OH^-, due to rapid PT to the latter. The $\Delta G°'$ value associated with a PT step can be calculated from:

$$-\Delta G = 0.05916(\mathrm{p}K_a - \mathrm{pH})\ \mathrm{eV} \qquad (7)$$

Using the average pK_a = 6.0 for a_4LRu^{II}−H^+MbFe^{IV}═O (Table 2) and the literature pK_a of 8.93 for $HHMbFe^{III}$−OH_2[34] yields $\Delta G°'$ values of 0.059 and −0.126 eV for the PT steps before and after ET, respectively. Thus, assuming the mechanism in eq 6a, the kinetic driving force for H^+MbFe^{IV}═O reduction to $MbFe^{III}$−OH^- is 0.829 eV, which is 0.067 eV lower than the reported thermodynamic potential of 0.896 eV.[33a] Therefore, the kinetic driving force for $Ru^{II} \rightarrow Fe^{IV}$═O ET in eq 6a (Table 2) is also 0.067 eV lower than the thermodynamic driving force.

Reorganization Energy for $Ru^{II} \rightarrow Fe^{IV}$═O ET. Marcus theory predicts that the rate constant for ET (k_{ET}) within a precursor complex is given by:[35]

(25) (a) Takano, T. *J. Mol. Biol.* **1977**, *110*, 569. (b) Phillips, S. V. E. *J. Mol. Biol.* **1980**, *142*, 531. (c) Kuriyan, J.; Wilz, S.; Karplus, M.; Petsko, G. A. *J. Mol. Biol.* **1986**, *192*, 133.
(26) Evans, S. V.; Brayer, G. D. *J. Mol. Biol.* **1990**, *213*, 885.
(27) Lambright, D. G.; Balasubramanian, S.; Decatur, S. M.; Boxer, S. G. *Biochemistry* **1994**, *33*, 5518.
(28) Shikama, K. *Coord. Chem. Rev.* **1988**, *83*, 73.
(29) Morikis, D.; Champion, M. P.; Springer, B. A.; Sligar, S. G. *Biochemistry* **1989**, *28*, 4791.
(30) Tian, W. D.; Sage, J. T.; Champion, P. M. *J. Mol. Biol.* **1993**, *233*, 155.
(31) Johnson, K. A.; Olson, J. S.; Phillips, G. N., Jr. *J. Mol. Biol.* **1989**, *207*, 459.
(32) Brantley, R. E., Jr.; Smerdon, S. J.; Wilkinson, A. J.; Singleton, E. W.; Olson, J. S. *J. Biol. Chem.* **1993**, *268*, 6995.
(33) (a) He, B.; Sinclair, R.; Copeland, B. R.; Makino, R.; Powers, L. S.; Yamazaki, I. *Biochemistry* **1996**, *35*, 2413. (b) George, P.; Irvine, D. H. *Biochem. J.* **1954**, 58, 188.
(34) George, P.; Hanania, G. I. H. *Biochem. J.* **1952**, *52*, 517.
(35) Marcus, R. A.; Sutin, N. *Biochim. Biophys. Acta* **1985**, *811*, 265.

$$k_{ET} = (4\pi^3/h^2\lambda k_B T)^{1/2}(H_{AB}) \exp[-(\Delta G^\circ + \lambda)^2/4\lambda k_B T] \quad (8)$$

The reorganization energy (λ) for the ET step can be calculated from eq 8. As has been previously stated,[14] the efficiency of ET between His48 and the heme in HHMb and SWMb appears to be identical, so the tunneling matrix element (H_{AB}) reported for SWMb (0.01 cm^{-1})[10,11] is adopted here. Using the $-\Delta G^\circ$ values estimated in the previous section (Table 2) and assuming $k_{ET} = k_2$ (eq 6a) results in $\lambda = 1.8$ eV for $Ru^{II} \rightarrow Fe^{IV}{=}O$ ET in the a_4IsnRu and a_4PyrRu derivatives, but $\lambda = 2.1$ eV for the a_5Ru derivative. Since λ is not expected to vary significantly between the three Mb derivatives, the much larger value in the latter suggests that ET is strongly gated at the higher driving force. A Marcus plot of ln k_{ET} vs $-\Delta G^\circ$ with $\lambda = 1.8$ eV (Figure 7) reveals that k_{ET} for the a_5Ru complex should be over 10-fold higher than the observed k_2 value of 3.6 s^{-1} (Table 2).

The generation of a negatively-charged oxo ligand ($Fe^{III}{-}O^{2-}$) in the hydrophobic heme pocket of Mb is likely to be highly unfavorable; hence, the oxene ligand is expected to be partially protonated in the precursor complex for ET. FTIR, resonance Raman, and kinetic studies have revealed that multiple open- and closed-pocket forms of $MbFe^{II}{-}CO$ exist.[29,30,36] Thus, it is conceivable that ET is gated due to the formation of a precursor complex in which a distal group is strongly H-bonded to the oxene ligand. The positively-charged guanidinium side chain of the distal Arg48 in cytochrome *c* peroxidase (CCP)[37] (Figure 7b) or the distal Arg38 in horseradish peroxidase (HRP)[38] act as H-bond donors to the oxene ligands in these peroxidases. Furthermore, there is strong evidence that reduction of the $Fe^{IV}{=}O$ center in HRP compound II (HRP-II) is rapid only when the oxene ligand is H-bonded to a distal species. Resonance Raman studies show that in HRP-II ν(Fe−O) shifts from 776 to 788 cm^{-1} at alkaline pH, with a transition midpoint at pH ∼8.5.[39] The 776-cm^{-1} band has been assigned to a H-bonded $Fe^{IV}{=}O$ moiety and the 788-cm^{-1} band, being insensitive to deuterium exchange, to a non-H-bonded $Fe^{IV}{=}O$ group.[39] HRP-II is a kinetically competent one-electron oxidant (eq 1c) at low pH but not at high pH, with a transition midpoint at pH 8.6.[40] Since ν(Fe−O) of $MbFe^{IV}{=}O$ is high (797 cm^{-1}) compared to that of the peroxidases (745−779 cm^{-1}),[41] and the 797-cm^{-1} band is both insensitive to pH in the range 6−12 and to substitution of D_2O for H_2O,[42] H-bonding to the oxene ligand in $MbFe^{IV}{=}O$ is highly unlikely.

Terminal metal oxo groups have been proposed to possess the following resonance structures:[43]

$$M{=}\ddot{O}: \rightleftharpoons M^{-}{\equiv}O:^{+} \quad (9)$$

The resonance can be expected to lie more to the right in $MbFe^{IV}{=}O$ but to the left in the $Fe^{IV}{=}O$ forms of the peroxidases because of the trans ligand effect of the proximal histidine. This is H-bonded to a carboxylate side chain in the peroxidases (Figure 7b),[2] and to a peptide carbonyl group in Mb, giving rise to a less basic oxygen atom in the latter. We propose that $MbFe^{IV}{=}O$ resembles the nonreactive, alkaline form of HRP-II, and that a conformational change is required to generate a Mb species that corresponds to the acid or kinetically competent form of HRP-II, leading to conformational gating of ET at high driving force, which is also consistent with the low SKIE (1.4) observed for k_2 (Table 2).

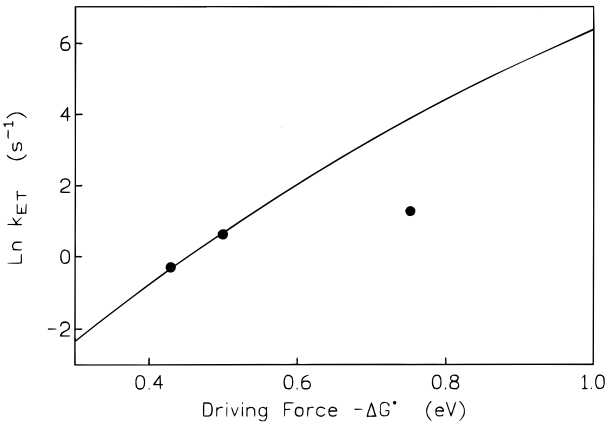

Figure 7. Plot of ln(k_{ET}) vs $-\Delta G^\circ$ (eV) for a_4LRuHis48Mb. Data were taken from Table 2 with $k_2 = k_{ET}$ (see text). The solid line represents the fit to the semiclassical Marcus equation for ET (eq 8) assuming $H_{AB} = 0.01$ cm^{-1} and a reorganization energy (λ) of 1.8 eV for ET between the Ru and heme centers.

A λ of 1.8 eV was calculated at lower driving forces for $Ru^{II} \rightarrow Fe^{IV}{=}O$ ET in the a_4LRu derivatives where ET must be rate limiting because of the sensitivity of k_{obs1} to $-\Delta G^\circ$ (Table 2 and Figure 7). It is of interest to compare this value with the λ (1.48 eV) reported for the intramolecular ET (a_5Ru^{II}-His48−$Fe^{III}{-}OH_2 \rightleftharpoons a_5R^{III}$His48−$Fe^{II} + H_2O$) in SWMb.[11] Considering that ET involves loss of the H_2O ligand and movement of the Fe with respect to the heme plane in $MbFe^{III}{-}OH_2$, the inner-sphere λ at the heme[44] was not expected to differ considerably from that associated with the ET in eq 6a. However, if the large Fe−O bond length change (0.2 Å) observed by EXAFS[45] on going from the oxene to the aquo ligand is taken into consideration, as well as the spin change on reduction of LS $Fe^{IV}{=}O$ ($S = 1$)[46] to HS $Fe^{III}{-}OH_2$ ($MbFe^{II}$ is also HS),[44] a ∼0.3 eV higher λ might not be unreasonable.

Conclusions. The results presented here would explain why $MbFe^{IV}{=}O$ is much less reactive toward one-electron reductants than compound II of heme peroxidases (eq 1c) at high $-\Delta G^\circ$. The requirement for H-bonding to the oxene ligand to generate a kinetically competent oxidant has been convincingly demonstrated for HRP-II.[39,40] The distal arginine of HRP,[38] CCP [37] (Arg 48 in Figure 7b), and other heme peroxidases[2] provides a strong H-bond donor to the oxene ligand. The lack of such a donor in its heme pocket under physiological conditions requires that $MbFe^{IV}{=}O$ must be converted to an activated form in a pH-dependent process prior to reduction. Furthermore, strong H-bonding to the proximal histidine ligand in the peroxidases (Figure 7b) would favor a resonance structure like that on the left of eq 9, with a considerably more basic oxygen atom than

(36) (a) Hong, M. K.; Braunstein, D.; Cowen, B. R.; Frauenfelder, H.; Iben, I. E. T.; Mourant, J. R.; Ormos, P.; Scholl, R.; Schulte, A.; Steinbach, P. J.; Xie, A.; Young, R. D. *Biophys. J.* **1990**, *58*, 429. (b) Doster, W.; Beece, D.; Bowne, S. F.; DiIorio, E. E.; Eisenstein, L.; Frauenfelder, H.; Reinisch, L.; Shyamsunder, E.; Winterhalter, K. H.; Yue, K. T. *Biochemistry* **1982**, *21*, 4831.

(37) (a) Fülöp, V.; Phizackerley, R. P.; Soltis, S. M.; Clifton, I. J.; Wakatsuki, S.; Erman, J.; Edwards, S. L. *Structure* **1994**, *2*, 201. (b) Miller, M. A.; Shaw, A.; Kraut, J. *Nature Struct. Biol.* **1994**, *1*, 524.

(38) Holzbaur, I. E.; English, A. M.; Ismail, A. A. *J. Am. Chem. Soc.* **1996**, *118*, 3354.

(39) Sitter, A. J.; Shifflett, J. R.; Terner, J. *J. Biol. Chem.* **1988**, *263*, 13032.

(40) (a) Critchlow, J. E.; Dunford, H. B. *J. Biol, Chem.* **1972**, *247*, 3714. (b) Dunford, H. B.; Stillman, J. S. *Coord. Chem. Rev.* **1976**, *19*, 187.

(41) Reczek, C. M.; Sitter, A. J.; Terner, J. *J. Mol. Struct.* **1989**, *214*, 27.

(42) Sitter, A. J.; Reczek, C. M.; Terner, J. *SPIE* **1989**, *1055*, 271.

(43) Kramarz, K. W.; Norton, J. R. *Prog. Inorg. Chem.* **1994**, *42*, 1.

(44) Tsukahara, K. *J. Am. Chem. Soc.* **1989**, *111*, 2040.

(45) Chance, M.; Powers, L.; Kumar, C.; Chance, B. *Biochemistry* **1986**, *25*, 1259.

(46) (a) Schulz, C. E.; Rutter, R.; Sage, J. T.; Debrunner, P. G.; Hager, L. P. *Biochemistry* **1984**, *23*, 4743. (b) Schulz, C. E.; Devaney, P. W.; Winkler, H.; Debrunner, P. G.; Doan, N.; Chiang, R.; Rutter, R.; Hager, L. P. *FEBS Lett.* **1979**, *103*, 102.

in the form on the right. It is of interest in this context that the solvent-exposed Fe^{IV}═O center of microperoxidase is observed to be an unreactive oxidant.[47] Presumably, the oxene ligand is very weakly basic, rendering the Fe^{IV}═O group unreactive around neutral pH.

CCP mutants are currently under preparation in our laboratory to study reaction 5 in a peroxidase chemical context. Surface residues close to the heme are being mutated to histidine to allow rapid $Ru^{II} \rightarrow Fe^{IV}$═O ET to be examined, and thereby determine the controlling factors in Fe^{IV}═O reduction in CCP.[48] The present results on $MbFe^{IV}$═O reduction suggest that the reactivity of the Fe^{IV}═O group is controlled by strong H-bonding to the oxene ligand and the proximal histidine. Such interactions would allow the local environment to determine the reactivity of Fe^{IV}═O catalytic intermediates in heme enzymes.

Acknowledgment. Research carried out at Concordia was supported by a grant from NSERC Canada to A.M.E. Research carried out at Brookhaven National Laboratory was under contract DE-AC02-76CH00016 with the U.S. Department of Energy and supported by its Division of Chemical Sciences, Office of Basic Energy Sciences. Professor Stan Brown (Queen's University) is thanked for helpful discussions.

JA963108G

(47) Low, D. W.; Winkler, J. R.; Gray, H. B. *J. Am. Chem. Soc*. **1996**, *118*, 117.

(48) English, A. M.; Fox, T.; Tsaprailis, G.; Fenwick, C. W.; Wishart, J. F.; Hazzard, J. T.; Tollin, G. In *Photochemistry and Radiation Chemistry: Complementary Methods for the Study of Electron Transfer*; Wishart, J. F., Nocera, D. G., Eds.; Advances in Chemistry Series; American Chemical Society: Washington, DC, in press.

(49) Sun, J.; Wishart, J. F.; Gardineer, M. B.; Cho, M. P.; Isied, S. S. *Inorg. Chem.* **1995**, *34*, 3301.